Engineering Journal issn: 0125-8281

Article

Erosion-Corrosion Simulation of Thermally Sprayed WC-Based Cermet in Artificial Seawater and Dam Water Environments

Muhamad Waldi[1,a,*], Ahmad M. Arkan Leksana[1], Helmi Bagas Samudra[1], Djoko Hadi Prajitno[1,2,b,*], Ekha Panji Syuryana[3], and Haris Tjahaya[4]

1 Department of Metallurgical Engineering, Faculty of Manufacturing Technology, Universitas Jenderal Achmad Yani, Bandung 40285, Indonesia
2 PRTNT National Research and Innovation Agency, Bandung 40132, Indonesia
3 Department of Mechanical Engineering, Faculty of Mechanical & Aerospace Engineering, Institut Teknologi Bandung, Bandung 40132, Indonesia
4 PT. Techno Spray Metalindo, Cikarang-Bekasi 17530, Indonesia

E-mail: [a,*]muhamad.waldi@lecture.unjani.ac.id (Corresponding author), [b,*]djok003@brin.go.id (Corresponding author),

Abstract. Mechanical equipment operated in a water dam environment is at risk of erosion-corrosion. To address this issue, thermally sprayed cermet coatings are an adequate solution for increasing resistance to corrosion and wear in hydro turbines, especially with high river sedimentation loads such as those in Cirata and Jatiluhur dams in Indonesia. In this study, WC-based cermet coatings with WC-10Co-4Cr and WC-12Co respectively were coated on AISI 1030 steel substrate and evaluated in media simulating the Cirata and Jatiluhur water dam environments, as well as in simulated seawater conditions. The morphology and structure of the sprayed coating were analyzed by SEM and XRD, and microhardness, porosity, and surface roughness were also studied. The corrosion resistance of the coating was evaluated using potentiodynamic polarization. More importantly, erosion-corrosion resistance in seawater simulations studied by Closed Flow Loop System (CFLS) equipment utilizing coupon tests was also explored. The results showed that the WC-10Co-4Cr coating has good electrochemical corrosion resistance with less erosion-corrosion compared to the WC-12Co coating, at 0.06-0.15 mm/year and 0.16-0.26 mm/year, respectively. Coatings with Cr content show a lower corrosion rate due to the formation of stable WCr_2O_6 and $W_{18}O_{49}$ oxides, making them a good choice for coating hydro turbine components.

Keywords: Coating, HVOF, erosion-corrosion, potentiodynamic, hydro-turbine.

ENGINEERING JOURNAL Volume 27 Issue 11
Received 19 August 2022
Accepted 17 November 2023
Published 30 November 2023
Online at https://engj.org/
DOI:10.4186/ej.2023.27.11.1

DOI:10.4186/ej.2023.27.11.1

1. Introduction

Corrosion is a phenomenon encountered in every aspect of life. Corrosion can change the properties of a material, decreasing its quality and reducing its service life [1–3]. Erosion-corrosion is the phenomenon of surface damage caused by high-velocity fluid and fluid pressure fluctuations, usually as the result of a shock or impact on components in contact with the fluid [4, 5]. It is a mechanism of damage encountered in hydro turbine components, causing material losses [6].

On the other hand, mechanical wear also greatly increases the corrosion rate. With increasingly severe working conditions, metal components may interact and become exposed to chloride (Cl^-) and even $SO4^{2-}$ ions and other corrosive media. Under similar erosion conditions, these media can cause more severe corrosion degradation [7, 8].

The solution to these problematic phenomena is to increase the thickness of a material by surface modification or coating deposition. Phase changes and changes in feedstock particle sizes can be modified as desired so that the coated material is protected and its service life increased [9, 10]. By combining coating processes and surface modifications on materials, their mechanical, physical, and chemical properties can be improved. Therefore, for this research achievement, a coating method known as thermal spray coating (TSC) was chosen in order to modify the metal surface by increasing its mechanical, physical, and chemical properties. High velocity oxy fuel (HVOF) spraying was used because the low porosity level of the obtained coatings provides good quality of spraying results [9, 11]

The most studied and applied cermet systems are coatings based on WC (WC-Co, WC-CoCr, WC-Ni) and CrC_2 (Cr_3C_2-NiCr, Cr_3C_2-Ni), due to their synergy and high levels of hardness and toughness. Carbide provides wear resistance, and resistance to impact. The application of tungsten carbide (WC) has been widely recognized as a reinforcement material with high wear resistance and low coefficient of friction. It has also been shown that some composite powders can produce coating deposits with unusual properties by optimally combining several material components[12-14]. Ludwig et al. showed that the WC-CoCr coating sprayed by the HVOF process increased erosion resistance under all test conditions because the HVOF coating increased wear resistance [12].

Compared with plasma spraying, HVOF spraying has a higher flame speed and lower flame temperature characteristics. Thus, the decomposition of WC can be reduced because the use of HVOF as a coating medium for WC-Co-based cermet powder will be better at dealing with erosion - corrosion in hydro turbine applications. Consequently, the use of cermet and HVOF applications is the best choice to mitigate these risks [15, 16]. In terms of coating microstructure and characteristics, HVOF provides a number of benefits that lead to increased performance in a variety of applications. This is especially true for coatings made of metal or cermet. HVOF have an outplay specific characteristics compared to other TSC technologies, for instances: particle velocity up to 800 m s^{-1}, relatively high bond strength, oxygen content in coatings between 1 to 5%, and low porosity level below 2%. Due to obvious improvements in characteristics, HVOF coatings are used today in a wide variety of industries. The main areas of application are industries where coatings are used to protect against wear, friction and corrosion [17, 18].

This study focuses on measuring the corrosion rate with mass loss using the coupon test method, and analyzing the severity of electrochemical corrosion for the WC-Co-based cermet coatings tested in dam water media and artificial seawater (NaCl 3.5%). While this kind of analysis has never been reported, knowledge of the corrosion rate and the mechanism of damage due to erosion-corrosion and its weight loss results could be of practical importance in the hydroelectric sector. In addition, electrochemical studies were carried out by water simulations of the Cirata Dam and Jatiluhur Dam for important hydroelectric power generation systems in West Java, Indonesia.

The substrate material chosen in this study is AISI 1030 steel. This material has been used for parts like shafts, gears, dowels, and other things where high strength is needed, but ductility also plays a crucial role in how well they work over time. Because of its superior hot formability features and cold forming capabilities, it has also been utilized for heavy-duty parts like pistons. This makes it appropriate for complex geometries when forming operations are required during the production process so that they can also be fabricated into drive shafts, axles, transmissions, and other hydro turbine parts.

2. Model and Method

2.1. Materials and Coatings

This research used two different coatings materials, WC-10Co-4Cr and WC-12Co, which were thermally sprayed. The powder used was a commercial, spherical, agglomerated, and sintered material from Praxair labeled 1350 VM for WC-10Co-4Cr, and Castolin Eutectic labeled 55588N for WC-12Co. The catalog of powders declared the nominal particle size distribution in the range of 11-16 μm, with the chemical composition of the spray shown in Table 1.

Table 1. Chemical composition (wt%) of cermet materials.

Coating	WC10Co4Cr	WC12Co
Chemical Composition	86% WC- 10%Co-4%Cr	88% WC-12%Co

TSC was deposited on AISI 1030 substrate, which chemical composition (according to the supplier) is shown in Table 2. The sample was cut from the plate shape to a size of 40 mm × 25 mm × 4 mm for erosion-

corrosion testing. For adhesion tests, sample was a AISI 1030 round bar with 25.4 mm in diameter and 38.1 mm in height. The sample was fabricated according to ASTM C633 standard.

Table 2. Chemical composition of the AISI 1030 substrate (wt.%).

Chemical Composition (wt.%)				
Fe	Mn	S	C	P
98.6 - 99.1	0.6 - 0.9	≤ 0.05	0.27 - 0.34	≤ 0.04

The carbon steel substrate was sandblasted with aluminium oxide (Al_2O_3) #16 grit prior to coating. Facilities from PT. Techno Spray Metalindo were used for thermal spraying of WC-CoCr and WC-Co cermet powders, while the equipment used for the HVOF thermal spray process was a HipoJet 2700 HVOF gun, with propane (C_3H_8) and oxygen as fuel. The spraying parameters are shown in Table 3. In all cases the orientation of the spray gun was perpendicular to the substrate (90°). The coating thickness was controlled in the range of 250-300 μm.

Table 3. Spraying parameters employed in the HVOF process

Parameters	Value
Spray distance (mm)	300
Pre-heating temperature of substrate (°C)	100
Speed of the feeder (rpm)	6.54 – 7.1
Gun tilt (°)	90
Fuel pressure C_3H_8 (kg cm^{-2})	75
Oxygen pressure (kg cm^{-2})	150
Air pressure (kg cm^{-2})	75
N_2 gas carrier (kg cm^{-2})	60
Thickness of coating (μm)	250-300

2.2 Characterization of the Coating

Microstructural analysis was carried out to study porosity, grain morphology, and oxide inclusions. The samples were prepared as follows: the cross section of the coating sprayed on the carbon steel substrate was cut and fixed in the epoxy resin. After that, the sample was sanded with silica paper with 80, 320, 800, and 1200 mesh. The sample was also polished with 6 μm diamond particles. Oxford X-act scanning electron microscope (SEM) Zeiss Evo 10 with energy dispersion spectroscopy (EDS) was used to evaluate the microstructure of sprayed coatings after corrosion testing treatment. Porosity levels were estimated by analysis using a 200× SEM micrographs in Image-J software version 1.8.0 with different levels of color contrast to distinguish the results of cermet deposits and porosity. The aim of the measurement was to determine the volumetric porosity levels (in %) in accordance with ASTM E2109-01 standard [19]. The software was able to calculate the volumetric porosity levels statistically. The powder phase characterization of HVOF coatings after corrosion testing was carried out using X-ray diffraction (XRD) by the analytical diffractometer Rigaku MiniFlex.

Microhardness was measured on a polished cross section of the thermal sprayed coating using the Vickers microhardness test instrument ZwickRoell Indentec under a load of 300 gf with dwelling time 10 seconds in accordance with ASTM E384. As many as 3 points for each type of coating were collected and averaged for hardness values. The adhesion test followed the ASTM C633 standard with 5 pair of samples glued using FM-1000 adhesive. FM-1000 adhesive cured in the furnace at a temperature of 250 °C for 1 hour. The sample was mounted on a jig and tested on Hung Ta (HT-8503) hydraulic tensile test machine capacity 100 kN.

2.3 Corrosion Test

The corrosion tests were performed by potentiodynamic polarization experiments in a three-electrode corrosion cell with a silver/silver chloride electrode (Ag/AgCl, sat.KCl) as the reference electrode (RE). In order to obtain uniform current distribution, a platinum (Pt) rod counter electrode was inserted into the cell. The samples were prepared as follows: a rectangular sample sheet was cut to size 1 cm x 1 cm, chemical cleaning was carried out in accordance with ASTM G1 Standard Practice for Preparing, Cleaning, and Evaluating Corrosion Test Specimens, which the backside of the specimens was covered with protective resin. The results were plotted in the Tafel diagram (log j - E). The corrosion potential (E_{corr}) and corrosion current density (j_{corr}) were determined according to Tafel equation and calculation of the corrosion rate followed ASTM G102 Standard Practice for Calculation of Corrosion Rates and Related Information from Electrochemical Measurements. Measuring instrument CorrTest Electrochemical and Corrosion Studio 5 was used to generate the polarization curve. Extrapolation of potentiodynamic polarization curve was used to obtain the j_{corr} and E_{corr} of the coating, indicating thus a severity of the corrosion process in artificial seawater (NaCl 3.5%) and dam water to simulate the conditions in both conditions. The open-circuit potential (OCP) of the samples was monitored for 15 min (enough time to stabilize the potential) followed by a dynamic change of polarization potential in the potential range of -300 mV OCP to +1200 mV versus OCP. versus reference electrode (RE), at the scan rate of 1 mV s^{-1}.

DOI:10.4186/ej.2023.27.11.1

Erosion-corrosion tests for both coatings were carried out with a closed flow loop system (CFLS) equipment in accordance with standard NACE RP 0775. Figure 1 shows the schematic of the CFLS. The sample was fixed using a holder, and the erosion-corrosion test was carried out in simulated artificial seawater (NaCl 3.5%).

The CFLS test utilized fluid flow system with a speed of 0.0278 L hour^{-1}, flow regime stratified, and temperature at ±45 ^{o}C. The measurement was done for each parameter, i.e., pH, E_{corr}, j_{corr} for every 24 hours over 5, 10, and 15 days. The samples were cleaned thoroughly after the test according to ASTM B117 using warm water and weighed after drying to quantified the weight loss. The weight loss was calculated as the corrosion rate in mm year^{-1} following the ASTM G1. Then the corrosion characteristics were investigated throughout 15 days of observation, with additional analysis carried out using SEM, and XRD to determine the morphology and the coating phase. The corrosion rate may then be obtained as follows:

$$CR = \frac{(K \times W)}{(A \times T \times D)} \quad (1)$$

where CR is corrosion rate (mm year^{-1}), K is constant, W is mass loss in grams, A area in cm^2, T is time exposure in hours, and D is material density in g cm^{-3}.

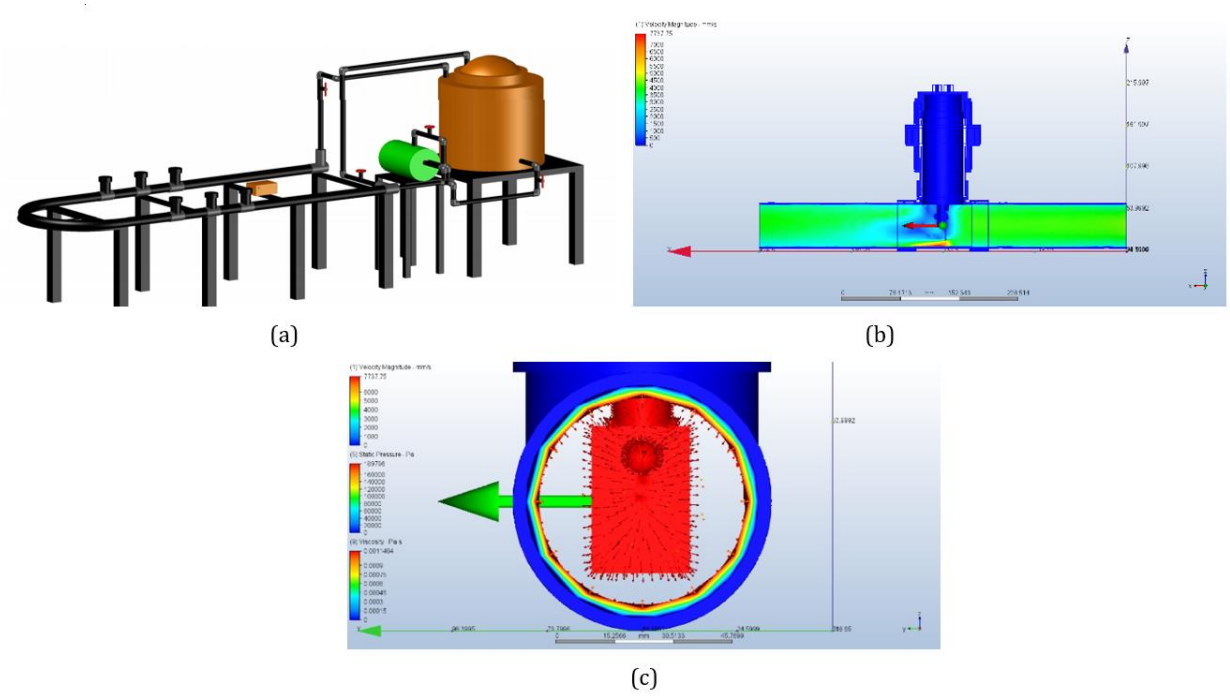

Fig. 1. Erosion-corrosion test simulation (a) Equipment of Closed Flow Loop System Testing (b, c) Internal condition with the arrow indicates the direction of the fluid and the specimen is in the holder with the orientation of the coating material facing the direction of the fluid.

3. Results and Discussion

3.1. Morphology and Microstructure Characterization of HVOF Thermal Spray Coatings

The coating thickness measurement of the WC-10Co-4Cr sample resulted by an average of 295.7 μm, while thickness measurement of WC-12Co by an average thickness of 289.72 μm. The measurement of coating thickness indicated several differences in the cross-section which could be caused by some factors, such as instability of spraying distance, velocity of the propelled materials, and the spraying angle [20, 21]

The micrographs showed that the splat patterns are similar to those found in previous research [22]. This indicates that with continuous spraying, the cermet droplets will impact the surface of the substrate and form a layered morphology distributed on the surface, and solidified into a lamellar structure. The un-melted particles were also identified, showing that their presence is strongly influenced by the parameters of the coating process, such as decline of combustion temperature, melting insufficiency of cermet powder during the combustion, inconsistency of propelled particle rate towards to the substrate, and rapid solidification of the particle along the transfer from spray gun to the surface. Oxide is also presented in minor amount.

The inconsistency of particle rate also greatly affects the melting of the feedstock powder when it propelled from the spray gun towards the substrate, so that it was solidified earlier before its strike the surface. A small part of the oxide also appears to form on the coating structure. All microstructure types of TSC commonly feature both melted and un-melted particles, as well as porosity as shown in the coating morphology (Fig. 2). The presence of porosity cannot be avoided during TSC

processing. Porosity has been caused by the air involvement supplied from fuel gas expansion and propelled the melted feedstock into splat. A relatively small part of free oxygen is involved in powder feed system, being trapped between the contact surfaces and causing porosity [23]. Detrimental effect of porosity in the coating is the reduced corrosion and erosion resistance [23, 24], bond strength of coating adhesion [26], and micro hardness [27]. Percentages of porosity of the two types of coatings, WC10Co4Cr and WC12Co, were 0.295% and 1.557%, respectively. In addition to the spraying process parameters, the existence of porosity is caused by large, globular cermet particles during the coating build up. When the cermet particles are large and globular, the thin droplets propelled from the spray gun break up on the surface and form a thin lamellar structure, stacked, and porosity created at each end of the lamellar particles [28].

Based on the surface hardness examination result, Table 4 shows that the WC-10Co-4Cr has a higher hardness value compared to WC-12Co. This explains that the addition of 4 wt.% Cr to WC-10Co-4Cr will increase the hardness value of the coating material. It can be seen that the microhardness value of the WC-10Co-4Cr coating has a value of 937.45 HV and WC-12Co has a value of 909.16 HV, which is respectively 529.16% and 510.17% greater than the substrate's hardness. This is mainly associated with coating buildup and the presence of large number of two kinds of tungsten carbide phases WC and W_2C [29].

Both WC-10Co-4Cr and WC-12Co show the presence of WC and W_2C hard carbide phases, and the results showed higher percentage value of W_2C than WC phase. This is because WC will decompose at high temperatures into W and C, forming the semicarbide phase (W_2C). At high temperature as a result of the HVOF spraying process, the following reactions will take place [30]

$$2WC \rightarrow W_2C + C \quad (2)$$

$$W_2C + ½\ O_2 \rightarrow W_2\,(C, O) \quad (3)$$

$$W_2\,(C, O) \rightarrow 2W + CO \quad (4)$$

Wood *et al.* 2018 [31] showed a decrease in the value of hardness of the WC-Co coating material with increasing levels of Co in the alloy. This is because the stability of the phase in the WC-Co phase equilibrium is increasing and the WC phase is decreasing, and therefore the level of hardness will decrease. This correlates with the WC-10Co-4Cr coating material. Also, the XRD results of the WC-10Co-4Cr coating material show that the WC and W_2C hard phases formed a total of seven peaks compared to the WC-12Co coating with only five peaks of the W-C hard phase formed. Thus, the hardness value will be proportional to the formation of metal carbide. Table 4 summarizes the characteristics of coating quality including thickness, roughness index, hardness, porosity, and adhesion.

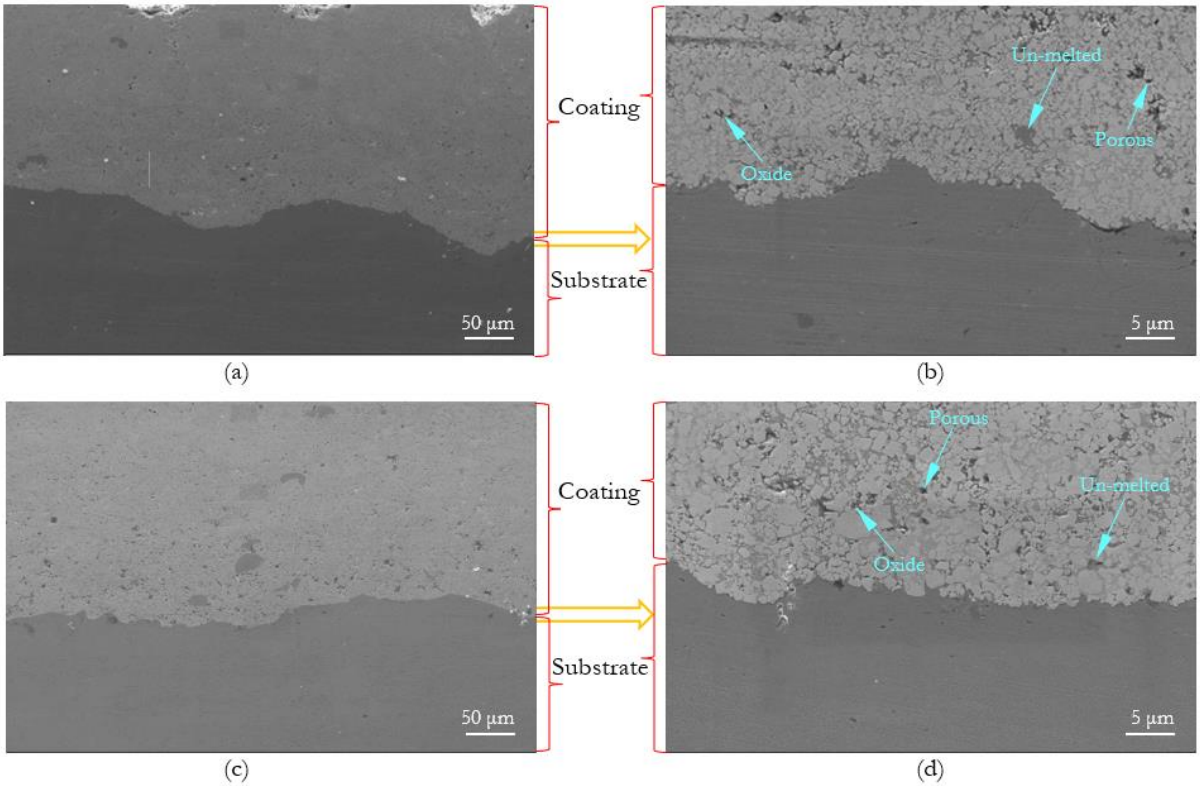

Fig. 2. Cross-section after HVOF TSC on AISI 1030 Steel 500x and 5000x Magnification. (a) & (b) WC-10Co-4Cr. (c) & (d) WC-12Co.

Table 4. Summary of quality characteristics data of HVOF thermal spray coating of WC-10Co-4Cr and WC-12Co coatings.

Coating specification	Coating thickness (μm)	Hardness value		Porosity level (%)	Roughness index (μm)	Adhesion (MPa)
		Substrate (HVN)	Coating (HVN)			
WC-10Co-4Cr	295.7	149	937,45	0.295	11.91	22.13
WC-12Co	289.72	149	909,16	1.557	10.49	21.36

3.2 Potentiodynamic Corrosion and Erosion-Corrosion Test by CFLS Method

The metal polarization curve consists of two reactions, namely a reduction reaction (cathode) and an oxidation reaction (anode). When the metal potential value becomes negative than the corrosion potential (E_{corr}) value, the metal undergoes a reduction reaction (cathode). Meanwhile, if the metal potential value becomes more positive than the E_{corr}, the metal undergoes an oxidation reaction (anode). In the oxidation reaction (anode) the metal is oxidized or releases electrons. E_{corr} and j_{corr} were extracted from the curve by the Tafel extrapolation method [9, 24]. Tafel diagrams generated from potentiodynamic polarization testing can also show the possibility of the formation of a passive layer above the oxidation potential value as shown in Fig. 3 where in every corrosion test and Table 5 describes the results obtained from Tafel curve processing.

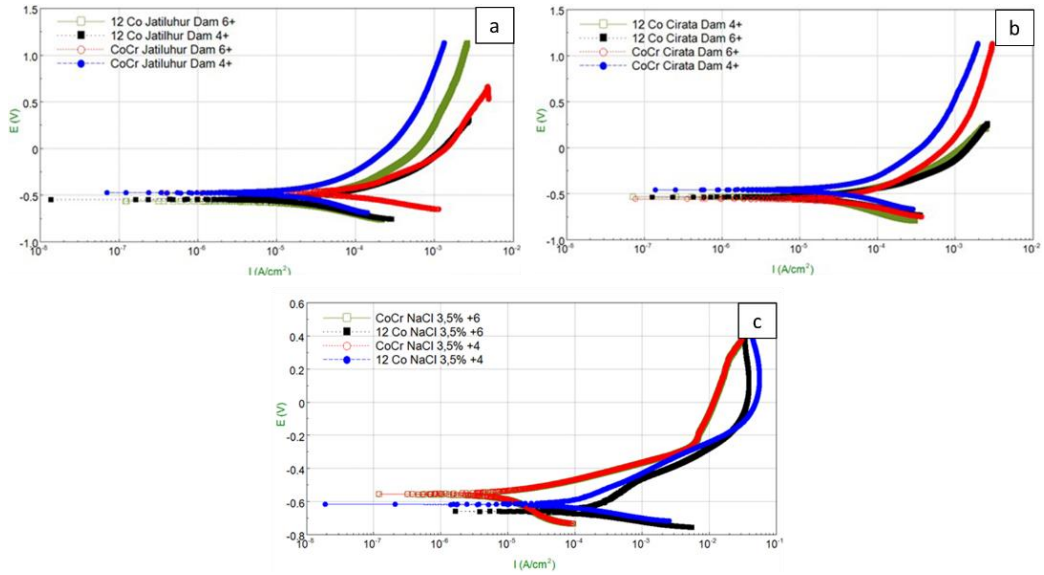

Fig. 3. Tafel polarization curves of cermet coatings in different test media: (a) Cirata Dam Water, (b) Jatiluhur Dam Water, (c) artificial seawater (3.5% NaCl).

Table 5. Results of Tafel curve data processing

Testing media	Parameters	Specimen test			
		WC-10Co-4Cr		WC-12Co	
		Valency +4	Valency +6	Valency +4	Valency +6
Cirata Dam Water	Anodic Tafel slope βa (mV dec^{-1})	23.582	12.454	63.999	47.534
	Cathodic Tafel slope βc (mV dec^{-1})	14.87	10.022	72.667	67.421
	j_{corr}, (mA cm^{-2}) × 10^{-3}	2.9254	2.0788	9.8273	8.7331
	E_{corr} *vs.* Ag/AgCl, (mV)	-460.21	-560.51	-531.715	-538.82
	Corrosion rate (*mm year*$^{-1}$)	0.13	0.07	0.43	0.26
Jatiluhur Dam Water	Anodic Tafel slope βa (mV dec^{-1})	18.82	5.242	58.335	65.919
	Cathodic Tafel slope βc (mV dec^{-1})	21.702	6.818	72.918	44.994
	j_{corr}, (mA cm^{-2}) × 10^{-3}	1.7781	2.1436	7.8781	5.6405
	E_{corr} *vs.* Ag/AgCl, (mV)	-477.47	-481.73	-548.18	-548.18
	Corrosion rate (*mm year*$^{-1}$)	0.08	0.06	0.34	0.16
Artificial seawater NaCl 3.5%	Anodic Tafel slope βa (mV dec^{-1})	30.774	36.887	14.8	10.081
	Cathodic Tafel slope βc (mV dec^{-1})	80.429	42.508	17.621	6.011
	j_{corr} (mA cm^{-2}) × 10^{-3}	4.0851	3.2611	5.2199	5.8581
	E_{corr} *vs.* Ag/AgCl, (mV)	-556.92	-556.93	-618.6	-661.03
	Corrosion rate (*mm year*$^{-1}$)	0.19	0.15	0.23	0.18

As shown in Table 5, the E_{corr} of the WC-10Co-4Cr coating material was more positive than the WC-12Co coatings in both dam waters and artificial seawater (NaCl 3.5%). In conclusion, the WC-10Co-4Cr coating has proven to be nobler than WC-12Co coating, having more positive corrosion potential, and lower corrosion current density compared to WC-12Co coatings. This indicates that in both dam water conditions and in the artificial seawater (NaCl 3.5%), the corrosion process is more susceptible to WC-12Co coatings [6].

As depicted in Table 5 and Fig. 4, WC-12Co coating showed a greater corrosion rate compared to the WC-10Co-4Cr coating in each of corrosion test medium. This was generally expected, because the presence of Cr is favourable for the formation of thin oxide films, which increase corrosion resistance [32]. Therefore, these results indicate that the addition of Cr would increase the corrosion resistance of WC-10Co-4Cr coating, making it a suitable choice for hydro turbine components coatings from the electrochemical point of view. At the other side, WC-12Co coating is more susceptible to oxidation and corrosion than WC-10Co-4Cr, which would be limiting for its application in dam waters. Unlike the oxides formed on WC-12Co coating, the Cr_2O_3 protective oxide layer formed on WC-10Co-4Cr acts as a barrier against corrosion. Possible oxide formation reactions are occurring according to the following equations:

$$Cr + H_2O \rightarrow CrO + 2H^+ + 2e^- \quad (5)$$

$$2CrO + H_2O \rightarrow Cr_2O_3 + 2H^+ + 2e^- \quad (6)$$

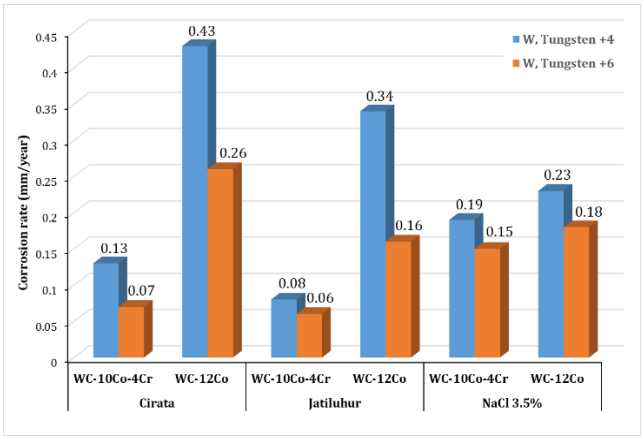

Fig. 4. Effect of different test media on corrosion rate of WC-based coatings generated from potentiodynamic polarization experiments.

Chrome-based oxide layer was also shown to appear in the XRD taken after corrosion test results in Fig. 5. Diffractogram of WC-10Co-4Cr coatings after the CFLS simulation (Fig. 5a) show the dominant formation of the $W_{18}O_{49}$ compound. Lee *et al.* in their research [33] stated that this compound has an attractive structure as an efficient ion carrier and more importantly, with the formation of these oxide compounds, high corrosion resistance to acidic environments is attained at lower potential values. The WC-12Co coating after the CFLS simulation (Fig. 5b) showed dominant result in the formation of WO_3 oxide, the possibility of the main reaction that occurred from dissolved tungsten oxidation for WC-10Co-4Cr coating was +4, or in a maximum state of corrosion. In contrast, the WC-12Co coatings was more in the possibility of dissolved oxidation being +6, or in a minimum state of corrosion. The passivation reactions are defined as following oxidation reactions [33]:

$$Co + H_2O \rightarrow CoO + 2H^+ + 2e^- \quad (7)$$

$$2W + 8OH^- + O_2 \rightarrow 2WO_3 + 4H_2O + 8e^- \quad (8)$$

$$3CoO + H_2O \rightarrow Co_3O_4 + 2H^+ + 2e^- \quad (9)$$

$$2WC + 3O_2 + 8OH^- \rightarrow 2CO_2 + 2WO_3 + 4H_2O + 8e^- \quad (10)$$

The Pourbaix diagram of tungsten in Fig. 6 shows that WO_4^{2-} state indicates a state of corrosion, while WO_3, W_5O_{14}, $W_{18}O_{49}$ and WO_2 are states of the passive layer formation that provide a protective barrier to the substrate.

Unlike potentiodynamic polarization test, the CFLS refers to the weight loss method for calculating the corrosion rate by monitoring differences of the coupon test specimen weights. Figure 6 shows that the WC-10Co-4Cr coating exhibits superior erosion-corrosion resistance compared to the WC-12Co coating in artificial seawater (NaCl 3.5%). First, it can be explained that the hardness of the WC-10Co-4Cr layer is greater than that of the WC-12Co layer because the hardness has a great influence to increase erosion-corrosion resistance [9]. Second, the low dissolution rate or solubility of the tungsten oxide coupled with Cr in the formation of the passive film of the WC-10Co-4Cr layer will inhibit erosion-corrosion damage due to the solubility resistance of the passive layer, although the film stability of the passive layer and the re-passivation ability for the WC-10Co-4Cr layer and WC-12Co layer are both reduced under these conditions of severe erosion [6, 10, 21]. In addition, high hardness values result in high elastic modulus values and the fracture toughness layers with both WC-10Co-4Cr and WC-12Co is very important for increasing wear and erosion resistance, as shown by other researchers.

The value of fracture toughness is described in the research of R. Wood *et al.* [31] which correlates to the hardness value of a coating material. The previous discussion regarding the hardness WC-10Co-4Cr has the highest hardness value. The higher the hardness value of the coating material, the lower the fracture toughness value compared to WC-12Co, which has better fracture toughness due to a lower hardness value. However, the initiation of damage and propagation on the surface of the two coatings is the main failure mechanism in the erosion-corrosion process.

During erosion-corrosion, the fluid will hit the layer and cause the area around the specimen to have a

turbulent flow orientation (turbulence), with the possibility of the formation of water bubbles continuously impacting the surface of the layer, resulting in stress and plastic deformation with defects such as pores in the coating. When stress reaches a certain level, micro-cracks may occur, and defects such as pores allow the formation of craters in the layer, thereby initiating erosion-corrosion. In the resulting layer exfoliation, cracks from different directions merge, as was confirmed in the studies of Liu *et al.* [5] and Hong *et al.* [21]. Therefore, lower porosity increases the corrosion resistance of the coating. As seen in Table 4, the WC-10Co-4Cr coating has a lower percentage of porosity compared to the WC-12Co coating.

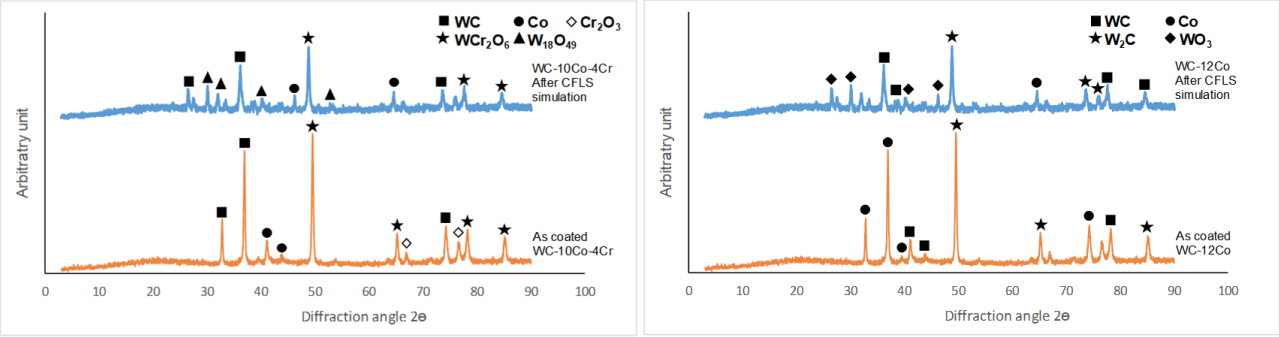

Fig. 5. Diffractograms of thermally sprayed coatings taken at two conditions *as-coated* and after CFLS simulation: (a) WC-10Co-4Cr, (b) WC-12Co.

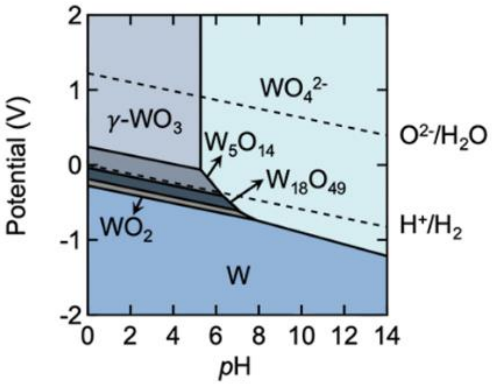

Fig. 6. Pourbaix diagram for tungsten system [34].

Pitting and crater formation were detected in the SEM observations at the cross-section of the layer in Fig. 8, after two cermet samples being exposed in artificial seawater (NaCl 3.5%) for 15 days (360 hours), confirming that mass loss begins at the micro-end and continues to expand until crater formation occurs. This phenomenon is in accordance with the results reported by other researchers [5, 29].

Figure 9 and Fig. 10 reveal SEM micrographs of TSC deposited WC-10Co-4Cr and WC 12 Co with back scattering feature which is capable to distinguish chemical elements of the coating after CFLS simulation. Figures show formation of a fairly high oxygen element content in both coatings at around 15±4 wt.%, whereby the tendency of tungsten to bind to oxygen is quite high compared to chloride in a NaCl environment so that the formation of tungsten oxide is shown as previously described [10]. NaCl has the opportunity to produce free chloride (Cl^-) because of the small size of the chloride atom so that it can diffuse into the coatings, causing pitting corrosion. the electrochemical test of the artificial seawater (NaCl 3.5%) has proven that chloride does diffuse in the coating system. This fluid flow-based test results in a higher corrosion rate due to the interaction of fluid flow loading with coating material so that the corrosion rate increased linearly. The results from the CFLS test in Fig. 7 indicate that the WC-10Co-4Cr coating has a lower erosion-corrosion rate than the WC-12Co coating.

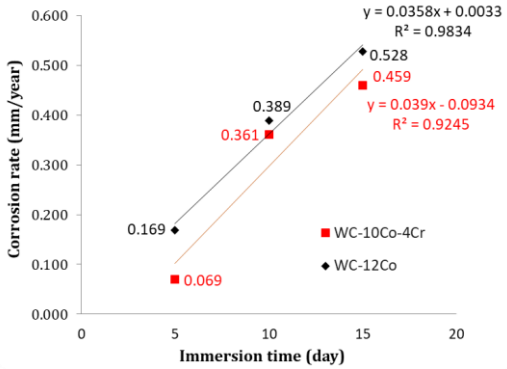

Fig. 7. Corrosion rate of cermet specimens with respect to immersion time in 3.5% NaCl solution.

Therefore, the relative corrosion rate was rated 0.459 mm $year^{-1}$ (*Good*) for the WC-10Co-4Cr coating up to 15 days of treatment, while the WC-12Co coating was rated at the same level (0.389 mm $year^{-1}$). This correlates to the results of electrochemical potentiodynamic polarization testing, where WC-based coatings with the addition of Cr showed a better effect on corrosion resistance and erosion-corrosion under environmental simulation tests. Therefore, it makes sense that WC-10Co-4Cr coatings should be used as an alternative protective coating for materials in hydro turbine applications because they have demonstrated better erosion-corrosion resistance, whereas WC-12Co coatings have limitations in this application. Table 6 classifies corrosion resistance based on the corrosion rate ranges.

Table 6. Relative corrosion resistance [35].

Relative corrosion resistance	Mils.yr^{-1}	mm.yr^{-1}	µm.yr^{-1}
Outstanding	< 1	< 0.02	< 25
Excellent	1 – 5	0.02 – 0.1	25 – 100
Good	5 – 20	0.1 – 0.5	100 – 500
Fair	20 – 50	0.5 – 1	500 – 1000
Poor	50 – 200	1 – 5	1000 – 5000
Unacceptable	200+	5+	5000+

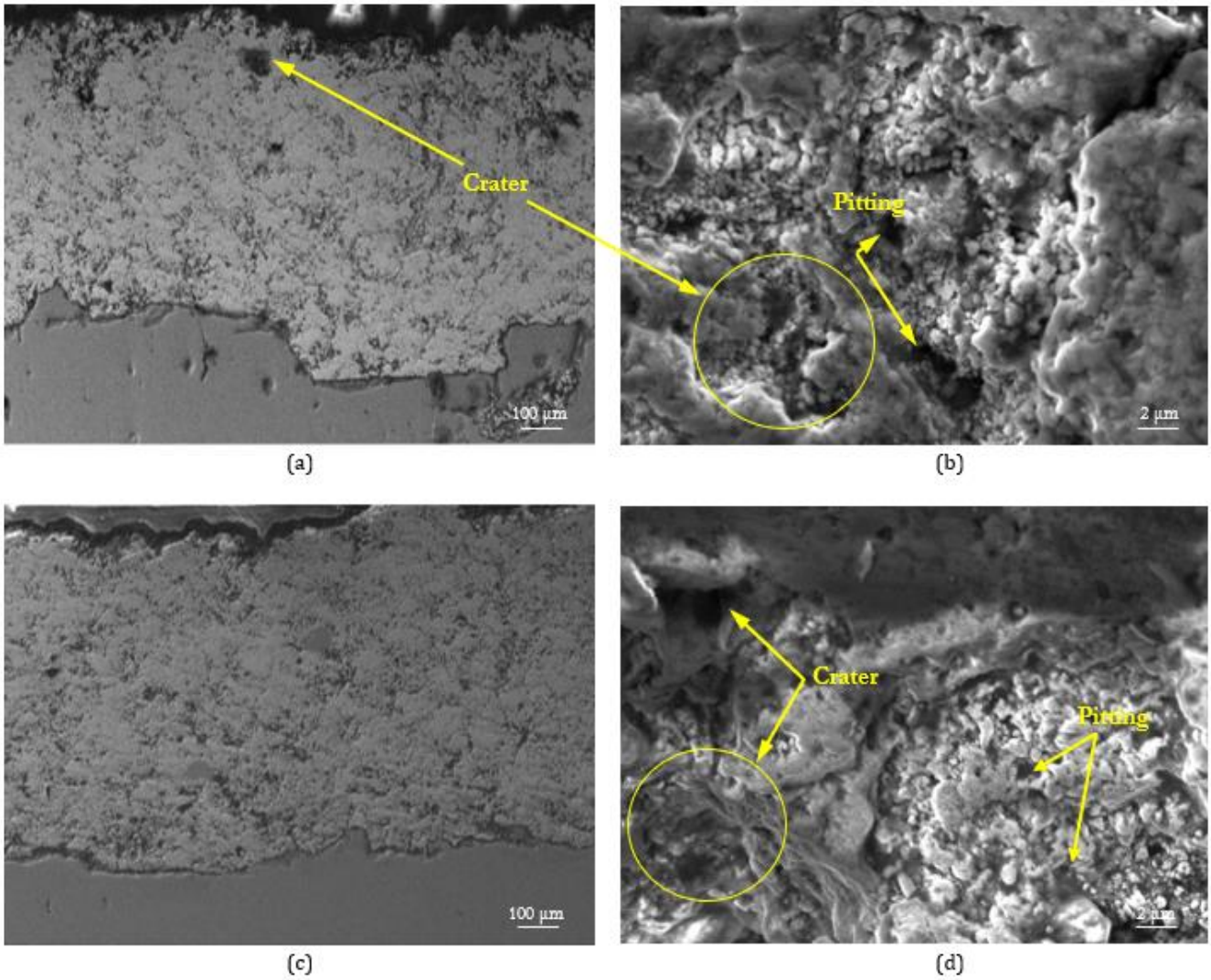

Fig 8. SEM images of WC cermet coatings after erosion-corrosion tests for 15 days in artificial seawater: (a) WC-10Co-4Cr 200× magnification (b) WC-10Co-4Cr 10,000× magnification (c) WC-12Co 200× magnification (d) WC-12Co 5000× magnification.

DOI:10.4186/ej.2023.27.11.1

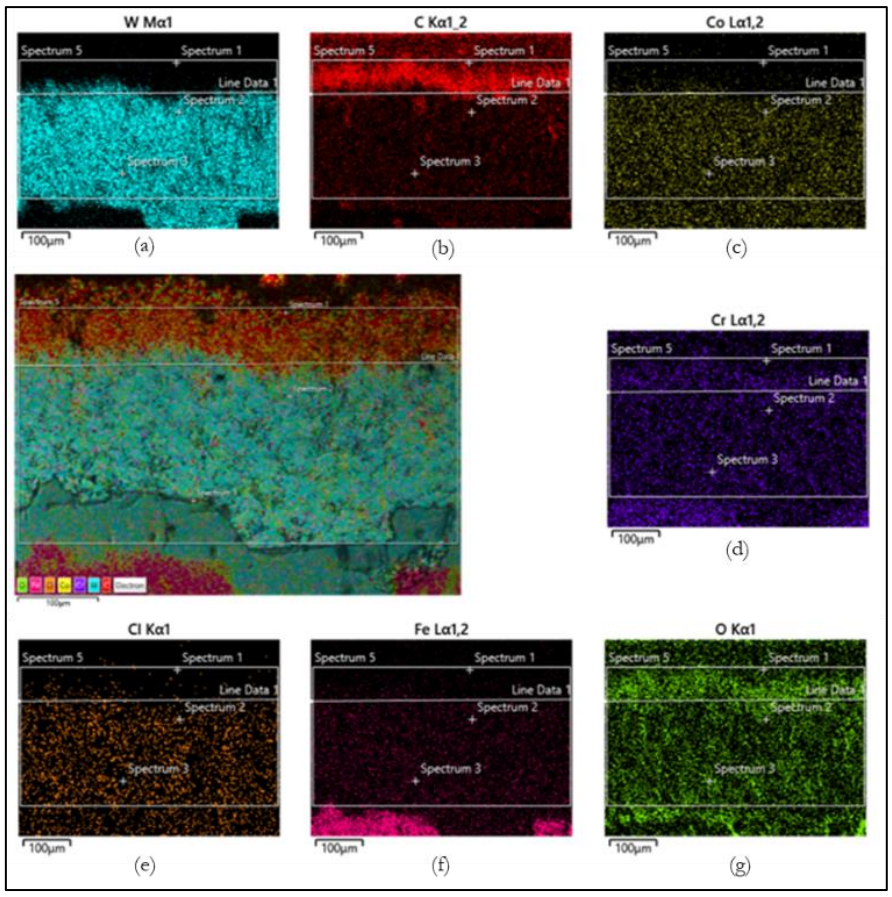

Fig 9. EDS test areas on SEM images (200× magnification) of WC-10Co-4Cr coating after corrosion test, showing distribution of elements in color form: (a) tungsten, (b) carbon, (c) cobalt, (d) chrome, (e) chloride, (f) iron, (g) oxygen.

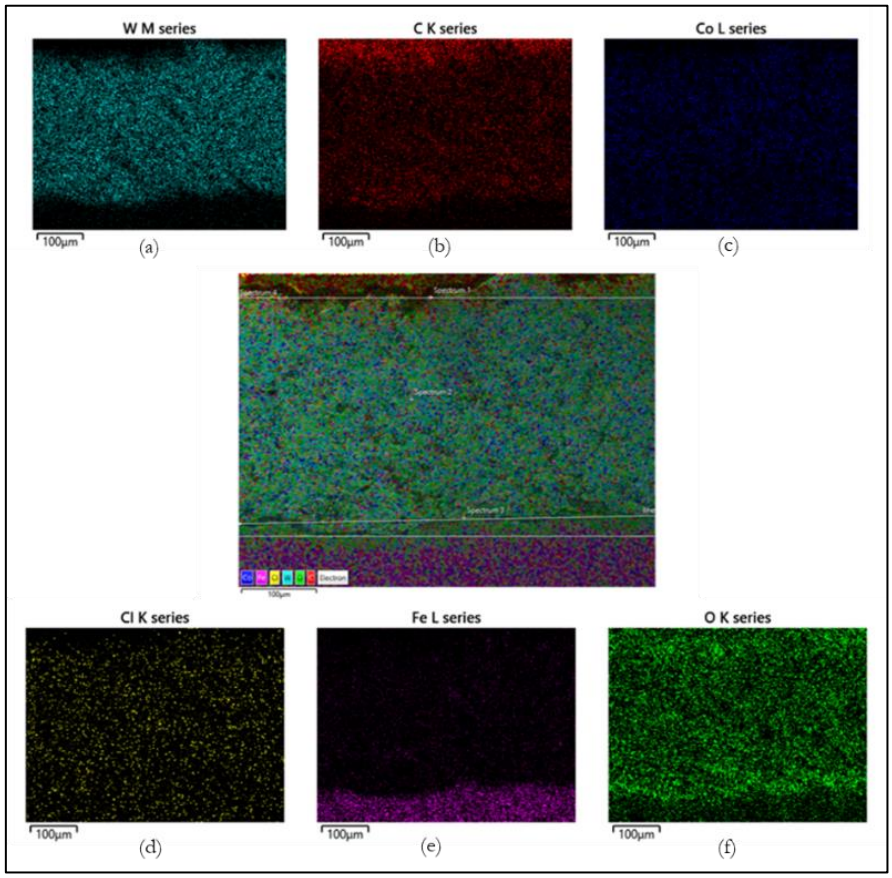

Fig. 10. EDS test area on SEM Results images (200X Magnification) of WC-12Co coating after corrosion test, showing distribution of elements in color form: (a) tungsten, (b) carbon, (c) cobalt, (d) chloride, (e) iron, (f) oxygen.

4. Conclusions

HVOF thermally sprayed WC-based cermet coatings (WC-10Co-4Cr and WC-12Co) important for hydro turbine application, increase resistance to erosion-corrosion process. The present research on WC-10Co-4Cr and WC-12Co coatings formed on AISI 1030 steel, has been conducted in order to study corrosion resistance, and erosion-corrosion reaction using potentiodynamic polarization and CFLS method, respectively. The following are the main conclusions that can be drawn:

1. Cermet WC-10Co-4Cr and WC-12Co coatings were successfully deposited by the HVOF technique. The coatings were uniform, adherent, free from cracks, and with minimum porosity less than 2%. Microhardness values were 937.45 HVN and 909.16 HVN, respectively.
2. Referring to the properties and characteristics of the second layer of cermet sprayed on AISI 1030 steel, WC-10Co-4Cr is found better than WC-12Co coating in all aspects of hardness, porosity, and corrosion resistance. This is because the addition of Cr in WC-10Co-4Cr has been shown to have a major effect on improving mechanical properties and corrosion resistance properties. Corrosion rate value of WC-10Co-4Cr is 0.06 - 0.15 mm year^{-1} was better than WC-12Co (0.16 - 0.26 mm year^{-1}). Corrosion rate based on potentiodynamic polarization measurements proves that corrosion phenomenon that occurs in WC-10Co-4Cr coating material has an *Excellent* corrosion resistance level and the corrosion rate tested for WC-12Co is *Good*.
3. Erosion-corrosion rate based on CFLS proves that WC-10Co-4Cr coating material has *Good* performance compared to WC-12Co. XRD has been identified to have an oxide passive layer WCr_2O_6 and $W_{18}O_{49}$ was formed on both coatings. However, due to the formation of the passive layer, the coatings were not optimal due to operational conditions involving dissoluble sedimentation of particles in the solution. Consequently, it is evident from the results of CFLS testing that the erosion-corrosion can reach a maximum level of 15 days of WC-10Co-4Cr is 0.459 mm year^{-1}, and 10 days of WC-10Co-4Cr is 0.389 mm year^{-1}.

Opportunity for improvement could be recommended by employing a post-spray treatment process such as sealing application and heat treatment to improve both mechanical properties and erosion-corrosion resistance of the coatings.

Acknowledgements

We are very grateful for the support from Dr. Djoko Hadi Prajitno of PRTNT National Research and Innovation Agency – Indonesia as main contributor, and PT. Techno Spray Metalindo for the equipment and materials provided for sample fabrication. The authors also declare that they have no conflict of interest.

References

[1] P. A. Schweitzer, *Fundamentals of Metallic Corrosion: Atmospheric and Media Corrosion of Metals*. CRC Press, 2007.

[2] V. Cicek and B. Al-Numan, *Corrosion Chemistry*. John Wiley & Sons, 2011.

[3] P. R. Roberge, *Handbook of Corrosion Engineering*. McGraw-Hill, 2000.

[4] P. Ponthiaux, F. Wenger, D. Drees, and J. P. Celis, "Electrochemical techniques for studying tribocorrosion processes," *Wear*, vol. 256, no. 5, pp. 459–468, Mar. 2004, doi: 10.1016/S0043-1648(03)00556-8.

[5] X. bin Liu *et al.*, "Cavitation erosion behavior of HVOF sprayed WC-10Co4Cr cermet coatings in simulated sea water," *Ocean Engineering*, vol. 190, Oct. 2019, doi: 10.1016/j.oceaneng.2019.106449.

[6] L. A. Luiz, J. de Andrade, C. M. Pesqueira, I. B. de A. F. Siqueira, G. B. Sucharski, and M. J. de Sousa, "Corrosion behavior and galvanic corrosion resistance of WC and Cr_3C_2 cermet coatings in madeira river water," *Journal of Thermal Spray Technology*, vol. 30, no. 1–2, pp. 205–221, Jan. 2021, doi: 10.1007/s11666-021-01152-8.

[7] H. Kumar, C. Chittosiya, and V. N. Shukla, "HVOF Sprayed WC based cermet coating for mitigation of cavitation, erosion & abrasion in hydro turbine blade," in *Materials Today: Proceedings*. Elsevier, 2018, pp. 6413–6420. doi: 10.1016/j.matpr.2017.12.253.

[8] S. Hong, Y. Wu, W. Gao, J. Zhang, Y. Zheng, and Y. Zheng, "Slurry erosion-corrosion resistance and microbial corrosion electrochemical characteristics of HVOF sprayed WC-10Co-4Cr coating for offshore hydraulic machinery," *Int J Refract Metals Hard Mater*, vol. 74, pp. 7–13, Aug. 2018, doi: 10.1016/j.ijrmhm.2018.02.019.

[9] Y. Liu, Z. Hang, N. Xi, H. Chen, C. Ma, and X. Wu, "Erosion-Corrosion Behavior of HVOF WC-Co Coating in Cl − and SO 42− Containing Solutions," *Appl Surf Sci*, vol. 431, pp. 55–59, Feb. 2018, doi: 10.1016/j.apsusc.2017.06.107.

[10] J. A. Picas, M. Punset, E. Rupérez, S. Menargues, E. Martin, and M. T. Baile, "Corrosion mechanism of HVOF thermal sprayed WC-CoCr coatings in acidic chloride media," *Surf Coat Technol*, vol. 371, pp. 378–388, Aug. 2019, doi: 10.1016/j.surfcoat.2018.10.025.

[11] S. W. Rukhande and W. S. Rathod, "Tribological behaviour of plasma and HVOF-sprayed NiCrSiBFe coatings," *Surface Engineering*, vol. 36, no.

7, pp. 745–755, Jul. 2020, doi: 10.1080/02670844.2020.1730062.

[12] G. A. Ludwig, C. F. Malfatti, R. M. Schroeder, V. Z. Ferrari, and I. L. Muller, "WC10Co4Cr coatings deposited by HVOF on martensitic stainless steel for use in hydraulic turbines: Resistance to corrosion and slurry erosion," *Surf Coat Technol*, vol. 377, Nov. 2019, doi: 10.1016/j.surfcoat.2019.124918.

[13] V. Matikainen, G. Bolelli, H. Koivuluoto, P. Sassatelli, L. Lusvarghi, and P. Vuoristo, "Sliding wear behaviour of HVOF and HVAF sprayed Cr_3C_2-based coatings," *Wear*, vol. 388–389, pp. 57–71, Oct. 2017, doi: 10.1016/j.wear.2017.04.001.

[14] Lech. Pawłowski, *The Science and Engineering of Thermal Spray Coatings*. Wiley, 2008.

[15] S. Rukhande, W. S. Rathod, and D. Bhosale, "Tribological behaviour of thermally sprayed coatings: A review," *Proceedings of TRIBOINDIA-2018 An International Conference on Tribology*, Dec. 2018, doi: http://dx.doi.org/10.2139/ssrn.3323697.

[16] E. Huttunen-Saarivirta, V. Heino, E. Isotahdon, L. Kilpi, and H. Ronkainen, "Tribocorrosion behaviour of thermally sprayed cermet coatings in paper machine environment," *Tribol Int*, vol. 142, Feb. 2020, doi: 10.1016/j.triboint.2019.106006.

[17] M. Oksa, E. Turunen, T. Suhonen, T. Varis, and S. P. Hannula, "Optimization and characterization of high velocity oxy-fuel sprayed coatings: Techniques, materials, and applications," *Coatings*, vol. 1, no. 1, pp. 17–52, Sep. 2011, doi: 10.3390/coatings1010017.

[18] A. S. M. Ang and C. C. Berndt, "A review of testing methods for thermal spray coatings," *International Materials Reviews*, vol. 59, no. 4, pp. 179–223, 2014. doi: 10.1179/1743280414Y.0000000029.

[19] M. Michalak, L. Łatka, P. Szymczyk, and P. Sokołowski, "Computational image analysis of suspension plasma sprayed YSZ coatings," *ITM Web of Conferences*, vol. 15, p. 06004, 2017, doi: 10.1051/itmconf/20171506004.

[20] G. Moskal, A. Tomaszewska, D. Migas, and D. Niemiec, "Cyclic oxidation resistance of Co-9Al-9W new cobalt-based superalloy," *Inżynieria Materiałowa*, vol. 40, no. 2, pp. 39–45, 2019, doi: 10.15199/28.2019.2.2.

[21] H. L. de Villiers Lovelock, P. W. Richter, J. M. Benson, and P. M. Young, "Parameter study of HP/HVOF deposited WC-Co coatings," *Journal of Thermal Spray Technology*, vol. 7, pp. 97–107, 1998, doi: https://doi.org/10.1007/s11666-006-5010-x.

[22] K. O. Méndez-Medrano, C. J. Martínez-González, F. Alvarado-Hernández, O. Jiménez, V. H. Baltazar-Hernández, and H. Ruiz-Luna, "Microstructure and properties characterization of WC-Co-Cr thermal spray coatings," *Journal of Minerals and Materials Characterization and Engineering*, vol. 06, no. 04, pp. 482–497, 2018, doi: 10.4236/jmmce.2018.64034.

[23] S. H. Zhang, T. Y. Cho, J. H. Yoon, M. X. Li, P. W. Shum, and S. C. Kwon, "Investigation on microstructure, surface properties and anti-wear performance of HVOF sprayed WC-CrC-Ni coatings modified by laser heat treatment," *Mater Sci Eng B Solid State Mater Adv Technol*, vol. 162, no. 2, pp. 127–134, May 2009, doi: 10.1016/j.mseb.2009.03.017.

[24] J. A. Picas, E. Rupérez, M. Punset, and A. Forn, "Influence of HVOF spraying parameters on the corrosion resistance of WC-CoCr coatings in strong acidic environment," *Surf Coat Technol*, vol. 225, pp. 47–57, Jun. 2013, doi: 10.1016/j.surfcoat.2013.03.015.

[25] A. Kumar, A. Sharma, and S. K. Goel, "Erosion behaviour of WC–10Co–4Cr coating on 23-8-N nitronic steel by HVOF thermal spraying," *Appl Surf Sci*, vol. 370, pp. 418–426, 2016, doi: 10.1016/j.apsusc.2016.02.163.

[26] T. Fiedler, R. Groß, J. Rösler, and M. Bäker, "Damage mechanisms of metallic HVOF-coatings for high heat flux application," *Surf Coat Technol*, vol. 316, pp. 219–225, Apr. 2017, doi: 10.1016/j.surfcoat.2017.03.037.

[27] S. Vignesh, K. Shanmugam, V. Balasubramanian, and K. Sridhar, "Identifying the optimal HVOF spray parameters to attain minimum porosity and maximum hardness in iron based amorphous metallic coatings," *Defence Technology*, vol. 13, no. 2, pp. 101–110, Apr. 2017, doi: 10.1016/j.dt.2017.03.001.

[28] M. Akhtari-Zavareh *et al.*, "Fundamentals and Applications of Thermal Spray Coating," *Canadian Journal of Basic and Applied Sciences*, vol. 05, pp. 1–11, 2017. [Online]. Available: https://www.researchgate.net/publication/322307359

[29] S. Hong *et al.*, "Microstructure and cavitation erosion behavior of HVOF sprayed ceramic-metal composite coatings for application in hydro-turbines," *Renew Energy*, vol. 164, pp. 1089–1099, Feb. 2021, doi: 10.1016/j.renene.2020.08.099.

[30] J. Nerz, B. Kushner, and A. Rotolico, "Microstructural Evaluation of Tungsten Carbide-Cobalt Coatings," *Journal of Thermal Spray Technology*, vol. 1, pp. 147–152, 1992, doi: https://doi.org/10.1007/BF02659015.

[31] R. J. K. Wood, S. Herd, and M. R. Thakare, "A critical review of the tribocorrosion of cemented and thermal sprayed tungsten carbide," *Tribol Int*, vol. 119, pp. 491–509, Mar. 2018, doi: 10.1016/j.triboint.2017.10.006.

[32] S. Hong *et al.*, "Cavitation erosion characteristics at various flow velocities in NaCl medium of carbide-based cermet coatings prepared by HVOF spraying," *Ceram Int*, vol. 47, no. 2, pp. 1929–1939, Jan. 2021, doi: 10.1016/j.ceramint.2020.09.022.

[33] S. Li *et al.*, "Corrosion behavior of HVOF sprayed hard face coatings in alkaline-sulfide solution," *Appl*

Surf Sci, vol. 416, pp. 69–77, Sep. 2017, doi: 10.1016/j.apsusc.2017.04.149.

[34] Y. J. Lee, T. Lee, and A. Soon, "Phase Stability Diagrams of Group 6 Magnéli Oxides and Their Implications for Photon-Assisted Applications," *Chemistry of Materials*, 2019, doi: 10.1021/acs.chemmater.9b01430.

[35] M. G. Fontana and Norbert D. Greene, *Corrosion Engineering*. McGraw-Hill, 2018.

Muhamad Waldi, is an assistant professor at the Department of Metallurgical Engineering, Universitas Jenderal Achmad Yani, Bandung – Indonesia. He obtained his bachelor degree from Universitas Jenderal Achmad Yani in 2003 and master degree at Institut Teknologi Bandung - Indonesia in 2018. He obtained an engineer profession from Universitas Parahyangan, Bandung – Indonesia in 2023. His research interests are high temperature materials, high temperature coatings, hot corrosion and welding technology. He's also a technical trainer; non-destructive examiner, assessor of various management system standards including quality, environmental, occupational health and safety, and educational organization.

Ahmad M Arkan Leksana, graduated with a bachelor degree from the Department of Metallurgical Engineering, Universitas Jenderal Achmad Yani, Bandung – Indonesia in 2021. During his studies, he actively joined the National Association Corrosion Engineer - student chapter (NACE - SC) at Universitas Jenderal Achmad Yani, as well as being a Laboratory Assistant Coordinator at the Chemical & Corrosion Laboratory of Metallurgical Engineering, Universitas Jenderal Achmad Yani.

Helmi Bagas Samudra, graduated with a bachelor degree from the Department of Metallurgical Engineering, Universitas Jenderal Achmad Yani, Bandung – Indonesia in 2021. During his studies, He actively joined as a research assistant in the National Nuclear Energy Agency, Bandung. He is now working at oil and gas industry as Production Engineer.

Dr. Djoko Hadi Prajitno is a senior researcher at Nuclear Research Center of National Research and Innovation Agency, Bandung – Indonesia and also active Lecturer at the Department of Metallurgical Engineering, Universitas Jenderal Achmad Yani, Bandung – Indonesia. He obtained bachelor degree in Mining Engineering of Institut Teknologi Bandung, master degree in Material Science and Engineering of University of New South Wales in 1996, and doctoral degree in Metallurgical Engineering of Institut Teknologi Bandung in 2013. His research interests are nuclear structural materials, corrosion, high temperature materials, high temperature coatings, and biomaterials.

Ekha Panji Syuryana is an Asset Integrity and Corrosion Engineer for scopes: oil, gas, geothermal, petrochemical and smelter industries with fourteen years experiences in the specific projects: surface and topside facilities, risk-based inspection (RBI), pipeline corrosion risk assessment and related asset integrity project. He obtained his bachelor degree from Universitas Jenderal Achmad Yani in 2008, master degree in Institut Teknologi Bandung in 2016, He obtained professional engineer from Intitut Teknologi Bandung in 2022. Recently, he is pursuing doctoral degree focusing flexible pipe material development at Mechanical Engineering Design of Intitut Teknologi Bandung. He was a former assistant professor at the Department of Metallurgical Engineering, Universitas Jenderal Achmad Yani, Bandung – Indonesia from 2016 to 2023. His research and professional interest in scope of corrosion of energy facilities to support asset integrity management system.

Haris Tjahaya is the CEO of PT Techno Spray Metalindo. The company providing thermal spray coating solution and service for mechanical component, including: rotating equipment, tubes, etc. He is also active member of Indonesian Coating Association (ASCOATINDO), and Metalworks and Machinery Industry (ASPEP).